Optimal Control of Tiltrotor Aircraft Following Power Failure

Yoshinori OKUNO§

National Aerospace Laboratory, Tokyo, Japan

and

Keiji KAWACHI†

*University of Tokyo, Tokyo, Japan*

Abstract

Optimal control of tiltrotor aircraft following power failure was theoretically studied using nonlinear optimal control theory. Optimization of the various take-off procedures, i.e., vertical, running, and oblique takeoffs in either a helicopter or conversion mode showed distinct advantages in increasing the maximum takeoff weight and/or decreasing the minimum takeoff distance, especially when applying variable critical decision speeds according to the takeoff field configuration. Optimal control procedures for landing and continued flight following power failure are also discussed with emphasis on the effects of nacelle angle control. The analytical method proposed in this paper is expected to contribute to more efficient use of tiltrotor aircraft in powered-lift transport category operations, and also considered to markedly reduce the cost, time, and risks involved in certification flight tests.

Abbreviations

AEO = all engines operating
BFL = balanced field length
CDP = critical decision point
CTO = continued takeoff
EF = engine failure
OAT = outside air temperature
OEI = one engine inoperative
R/C = rate of climb
RTO = rejected takeoff
V_{EF} = flight speed at engine failure
V_1 = critical decision speed
V_2 = takeoff safety speed

---

§ Researcher, Flight Research Division.
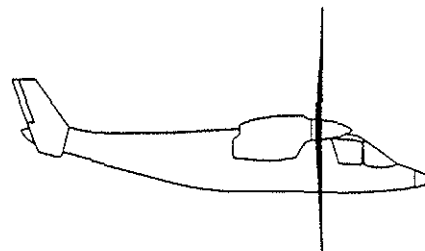† Professor, Department of Aeronautics.

Introduction

Tiltrotor aircraft have the capability to survive power failure, with their fly-away success and/or safe landing following power failure depending on several flight conditions at the moment of power failure, e.g., height and velocity (these limits are shown in a H-V diagram), and on the flight mode (Fig. 1). The cruising airplane mode, having the minimum power requirements, can normally be continued in a one-engine-inoperative (OEI) condition. In fact, even if all engines fail, by converting to the helicopter mode,
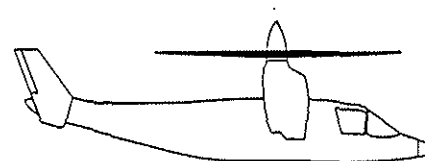
(a) Helicopter Mode
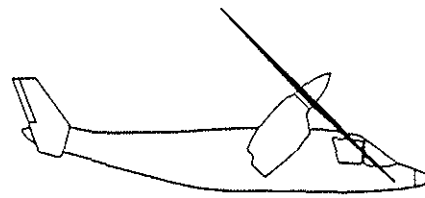
(b) Conversion Mode

(c) Airplane Mode

Fig. 1 Tiltrotor aircraft flight modes.

an autorotative landing can be performed if the initial height is sufficient for the transition. The effect of power failure is most critical when it occurs during takeoff, thus the takeoff weight, especially in transport category operations (Ref. 1), is often limited to insure safety following power failure.

Tiltrotor aircraft takeoff procedures include several variations as shown in Fig. 2. A vertical takeoff is used for zero-field-length operations from very confined areas, e.g., a roof-top vertiport, although the takeoff weight is most significantly limited so that a safe return to the original takeoff point is assured. In contrast, the running takeoff can bear a much heavier takeoff weight, even if the in-ground-effect (IGE) hover ceiling is exceeded, providing the runway length is adequate to handle both a continued and rejected takeoff. When using the oblique takeoff in either the helicopter or conversion mode, the maximum takeoff weight and required takeoff distance can be traded off according to the available takeoff field length.

These operational limitations have been verified for helicopters by certification flight tests, however, they require significant cost and effort due to the high risks involved and the various influential parameters. A theoretical method was subsequently developed to evaluate helicopter flight safety following power failure (Ref. 2) by applying nonlinear optimal control theory to improved dynamic and aerodynamic models. In the present paper, this method was extended for a tiltrotor configuration and then applied to the optimal control problems of tiltrotor aircraft following power failure, with emphasis on optimizing the takeoff procedures for transport category operations.

Formulation

Dynamic and Aerodynamic Models

Longitudinal three-degree-of-freedom motion is considered assuming a rigid-body dynamic model. The state variables are height above takeoff surface h, flight distance x, forward speed u, rate of descent w, pitch attitude Θ, pitch rate q, rotor rotational speed Ω, and nacelle angle i_n ($0°$ in the airplane mode and $90°$ in the helicopter mode). The control variables are blade collective pitch θ_0, nacelle angle rate q_n, and the pitching control moment M which can be substituted for a combination of the elevator angle and blade longitudinal cyclic pitch related to the nacelle angle. The equations of motion are given as follows:
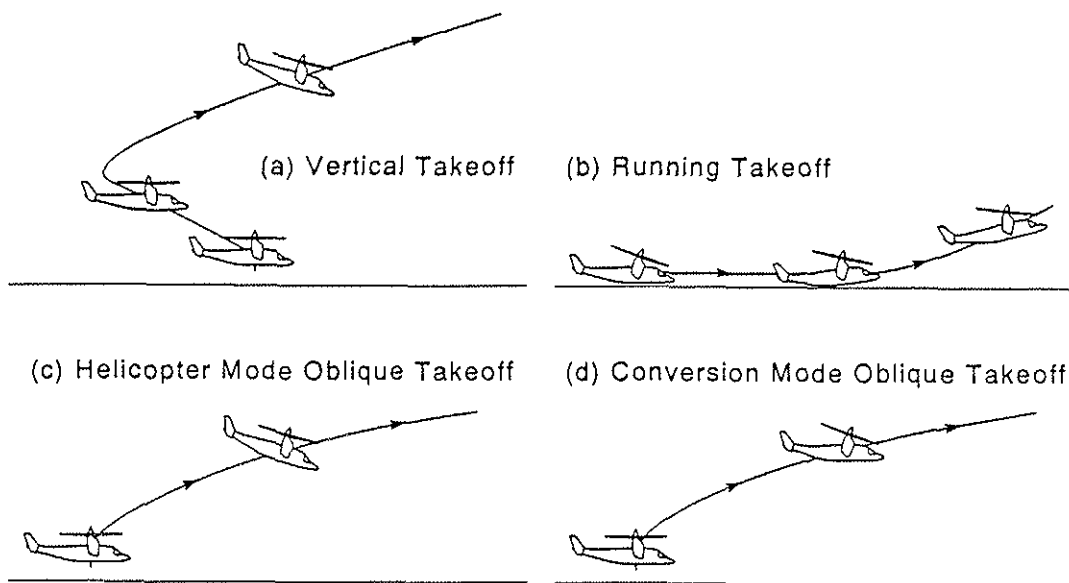
(a) Vertical Takeoff   (b) Running Takeoff

(c) Helicopter Mode Oblique Takeoff   (d) Conversion Mode Oblique Takeoff

Fig. 2   Tiltrotor aircraft takeoff procedures.

$$dh/dt = -w$$

$$dx/dt = u$$

$$du/dt = \{T\cos(\Theta + i_n) - H\sin(\Theta + i_n) \\ - L\sin\gamma - D\cos\gamma\}/m$$

$$dw/dt = -\{T\sin(\Theta + i_n) + H\cos(\Theta + i_n) \\ + L\cos\gamma - D\sin\gamma\}/m + g$$

$$d\Theta/dt = q$$

$$dq/dt = M/I_Y$$

$$d\Omega/dt = (Q_a - Q_r)/I_R$$

$$di_n/dt = q_n$$

where T, H and Q_r are respectively thrust, H-force and torque of the rotors, Q_a is available engine torque, L and D are fuselage lift and drag (including wing contribution), γ is flight path angle (positive climbing), m is aircraft mass, and I_R and I_Y are rotor moment of inertia and body moment of inertia with respect to pitching axis.

The rotors' aerodynamic performance was calculated using modified blade element theory in combination with modified momentum theory (Ref. 2). The former theory takes into account the effects of blade root stall during descent, being one of the most characteristic problems of tiltrotor aircraft due to their highly twisted rotor blades, whereas the latter theory is valid over the entire operating envelope including the vortex ring state. The airfoil's lift and drag coefficients were given by a function of the airspeed in order to take into account compressibility effects. The rotor thrust reduction due to the wing download was assumed by the following empirical equation:

$$T = T^* \left(1 - \frac{0.1}{\mu/0.025 + 1}\sin i_n\right)$$

where T^* is the isolated rotor's calculated thrust.

Typical assumed tiltrotor aircraft specifications are given in Table 1, being based on the XV-15 tiltrotor research aircraft. Figure 3 shows the required power variation of this tiltrotor aircraft with respect to flight speed and various nacelle angles, where the

results obtained using the presented dynamic and aerodynamic models show good agreement with the flight tests results (Ref. 3). The nacelle angle limitation due to wing stall was also analyzed (Fig. 4), and found to be in good agreement with the XV-15's conversion corridor (Ref. 4).

Table 1 Tiltrotor aircraft specifications

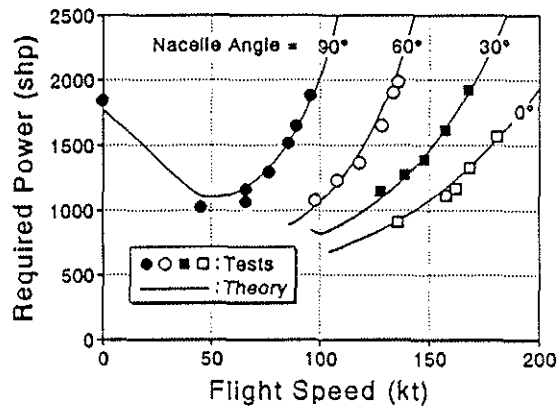|	
Maximum Gross Weight	15000 lbf
Empty Weight	10000 lbf
Rotor Radius	12.5 ft
Blade Chord	14.0 in
Rotor Design Speed (Helicopter/Conversion Mode)	565 rpm
Number of Blades	3
Wing Area	169 ft²
Wing Span	32.2 ft

Fig. 3 Required power variation with respect to flight speed for various nacelle angles.
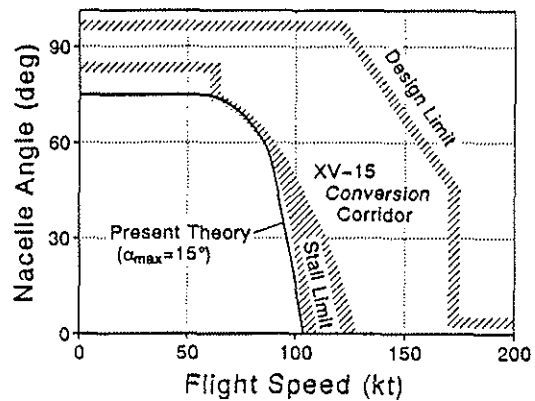

Fig. 4 XV-15 Conversion corridor.

Optimization Problems

Several optimization problems were formulated, e.g., maximizing the takeoff weight in VTOL operations and minimizing the required takeoff distance in STOL operations, with each problem's performance index and terminal conditions being discussed in subsequent sections. The initial conditions were established by the state variables 1 sec after power failure in order to simulate normal pilot reaction time. The allowable ranges of the control variables and some of the state variables were limited by the following inequality constraints:

$$\theta_{0\ min} \leq \theta_0 \leq \theta_{0\ max}$$

$$|M| \leq M_{max}$$

$$|q_n| \leq q_{n\ max}$$

$$\Theta_{min} \leq \Theta \leq \Theta_{max}$$

$$\Omega_{min} \leq \Omega \leq \Omega_{max}$$

$$i_{n\ min} \leq i_n \leq i_{n\ max}$$

These nonlinear optimal control problems with inequality constraints were numerically solved using "slack variables" (Ref. 5) and the Sequential Conjugate Gradient Restoration Algorithm (Ref. 6).

Optimal Control Procedures following Power Failure

Optimal control procedures following power failure during hover were studied with emphasis on nacelle angle control effects. Two typical cases were considered, i.e., continued flight (fly-away) following one engine failure and an autorotative landing following total power failure.

Fly-Away following Power Failure

The fly-away optimization problem was formulated so as to minimize the initial hovering height using the terminal condition of transition to level flight with 35 ft minimum clearance above the takeoff surface. The performance index and the terminal conditions

are given as

$$I = \min h(0)$$

where

$$h(t_f) = 35 \text{ ft}, \quad w(t_f) = 0$$

Here the maximum contingency power was assumed as 1250 shp, corresponding to the XV-15's maximum continuous power since it is a research aircraft and therefore designed to have excessive contingency power (1800 shp) for commercial aircraft use.

Figure 5 shows two optimal solutions assuming a fixed and optimally controlled nacelle angle. Optimal nacelle angle control is shown to reduce the height loss during transition by 15 % (27 feet) since it produces a high pitch attitude which contributes to increased wing lift.

Landing following Power Failure

The landing optimization problem following total power failure was formulated to minimize the initial hovering height (called high hover height) using the terminal condition that the touchdown speed factor, which is a sum of the squares of nondimensionalized forward speed and rate of descent at touchdown, is within the landing gear capacity as follows:

$$I = \min h(0)$$

where

$$h(t_f) = 0, \quad \left\{ u(t_f)/u_{max} \right\}^2 + \left\{ w(t_f)/w_{max} \right\}^2 \leq 1$$

As shown by the results in Fig. 6, the optimal nacelle angle control has little effect on the high hover height (5 %, 25 feet).

Optimization of Takeoff Procedures

Since the required takeoff distance is considered as the longer of the continued takeoff (CTO) and rejected takeoff (RTO) distances when power fails at the critical decision point (CDP) (Ref. 1), it is usually minimized in a balanced field length (BFL) condition where the CTO and RTO distances are equal.
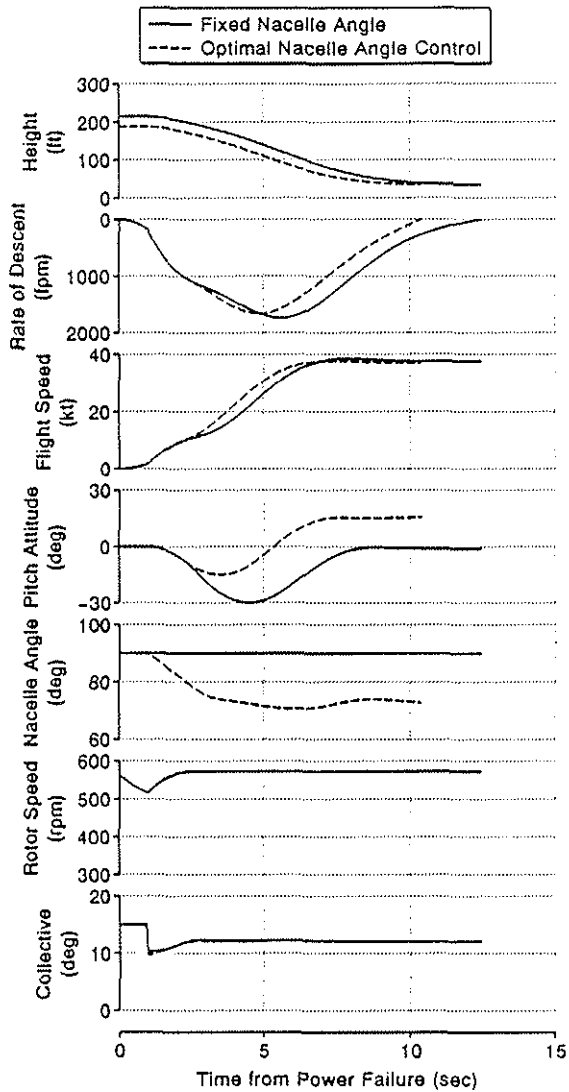
Fig. 5 Time histories of fly-away following one engine failure while hovering (W=12870 lbf).
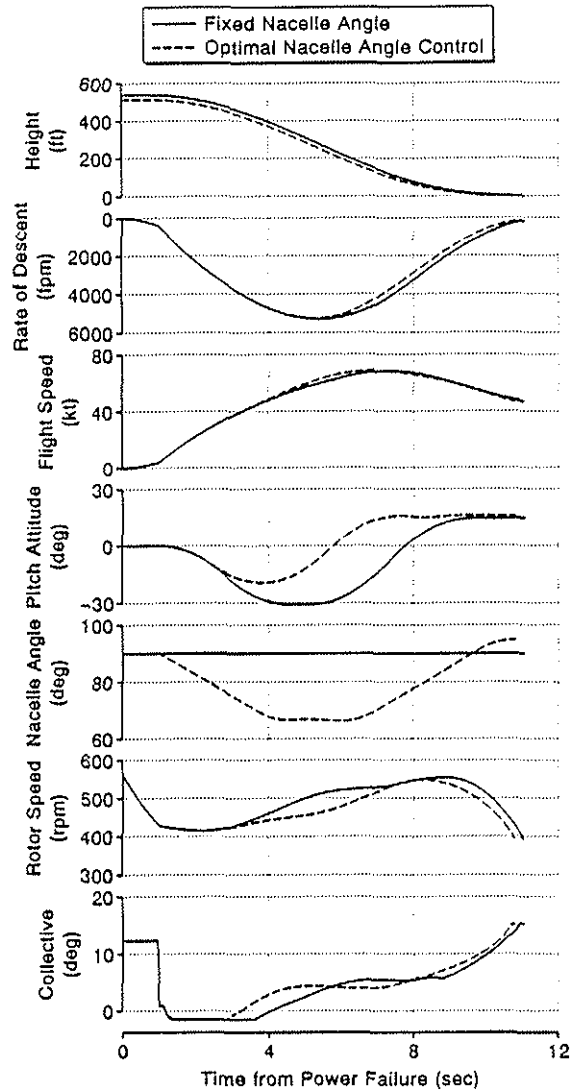

Fig. 6 Time histories of landing following total power failure while hovering (W=10000 lbf).

Here, the CTO distance is defined to be from the initial hovering point to the point complying with the following three requirements: minimum clearance of 35 feet above the takeoff surface, positive rate of climb, and attainment of the takeoff safety speed V_2 at which a 300 fpm minimum rate of climb is assured using the maximum OEI power. On the other hand, the RTO distance is the distance from the initial hovering point to a completely stopped point, and after touchdown being assumed to be given by $u(t_f)^2/(2 \cdot 0.2g)$, where a constant deceleration of $0.2g$ is assumed during the ground run.

Oblique Takeoff

The optimization problems for the helicopter/conversion mode oblique takeoff were formulated to minimize the CTO and RTO distances following power failure as follows:

For the CTO,

$$I = \min \ x(t_f)$$

where

$$h(t_f) \geq 35 \text{ ft}, \quad w(t_f) \leq 0, \quad u(t_f) \geq V_2$$

For the RTO,

$$I = \min \left\{ x(t_f) + u(t_f)^2/(2 \cdot 0.2g) \right\}$$

where

$$h(t_f) = 0, \; \left\{ u(t_f)/u_{\max} \right\}^2 + \left\{ w(t_f)/w_{\max} \right\}^2 \leq 1$$

The all-engines-operating (AEO) takeoff path until power failure was calculated using the following assumptions: 1) The pitch attitude during the helicopter mode takeoff and the nacelle angle during the conversion mode takeoff are assumed to be constant, with both being determined to minimize the required takeoff distance, whereas the pitch attitude during the conversion mode takeoff is assumed to be maintained level, 2) Transition from initial hover to these takeoff configurations was performed using the maximum pitching moment/nacelle angle rate in the helicopter/conversion mode takeoff, respectively, and 3) The AEO takeoff power is assumed as 2000 shp.

Figure 7 shows the optimal CTO and RTO paths for three takeoff procedures, i.e., a helicopter mode takeoff, conversion mode takeoff with fixed nacelle angle, and conversion mode takeoff with optimal nacelle angle control following power failure. The critical decision speed was optimized for each takeoff procedure so that the BFL condition is obtained. As shown by Fig. 7 (a) and (b), the BFL is nearly independent of the nacelle angle if fixed following power failure. When the critical decision speed has
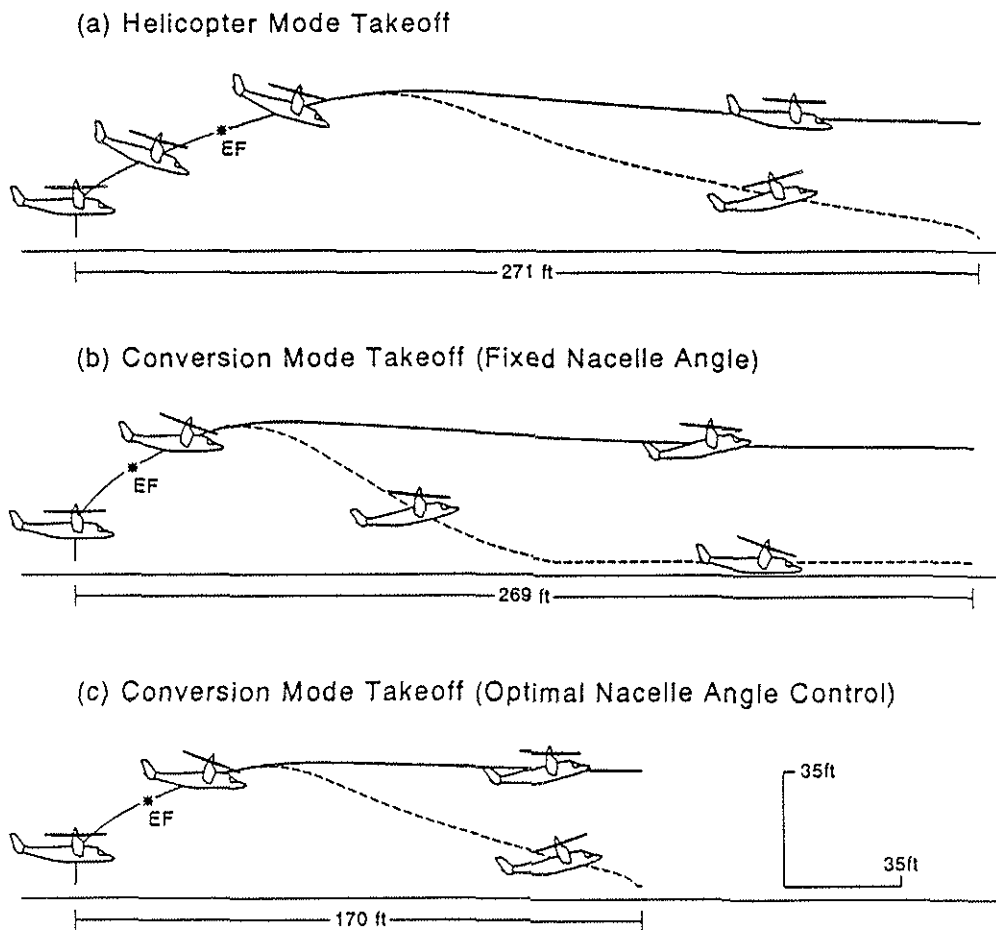
(a) Helicopter Mode Takeoff

271 ft

(b) Conversion Mode Takeoff (Fixed Nacelle Angle)

269 ft

(c) Conversion Mode Takeoff (Optimal Nacelle Angle Control)

170 ft

35ft

35ft

Fig. 7 Optimal continued and rejected takeoff paths for an oblique takeoff (W=12000 lbf).

238

a single value for both these takeoff procedures, the helicopter mode takeoff requires a shorter RTO distance than the conversion mode takeoff since a rapid deceleration is available using a pull-up maneuver, whereas it requires a longer CTO distance due to the increased power requirement caused by the negative pitch attitude.

Although the required takeoff distance is minimized in the BFL condition, the CTO and RTO distances can be traded off according to the takeoff field configuration as shown in Fig. 8. If the takeoff field is clear as in a riverside vertiport, the helicopter mode takeoff with a low critical decision speed requires a 38 % shorter runway than the BFL as shown in Fig. 8 (a) and (b). Here the minimum critical decision speed is limited by the requirement that the

height loss during the CTO must be less than half the critical decision height ($H_{EF}/2$). In contrast, if obstacles exist in the takeoff field as shown in Fig. 8 (c), the conversion mode takeoff using a high critical decision speed is preferable because of the short CTO distance.

Since fixed nacelle angles were assumed in the preceding discussions, the BFL decreases by 37 % if the nacelle angle is optimally controlled following power failure (Fig.7 (c)). Figure 9 shows the time histories of the CTO and RTO paths using optimal nacelle angle control. As can be seen from the nacelle angle history, the RTO's optimal nacelle angle control is a simple conversion to its upper limit, thus being easily performed by the pilot.
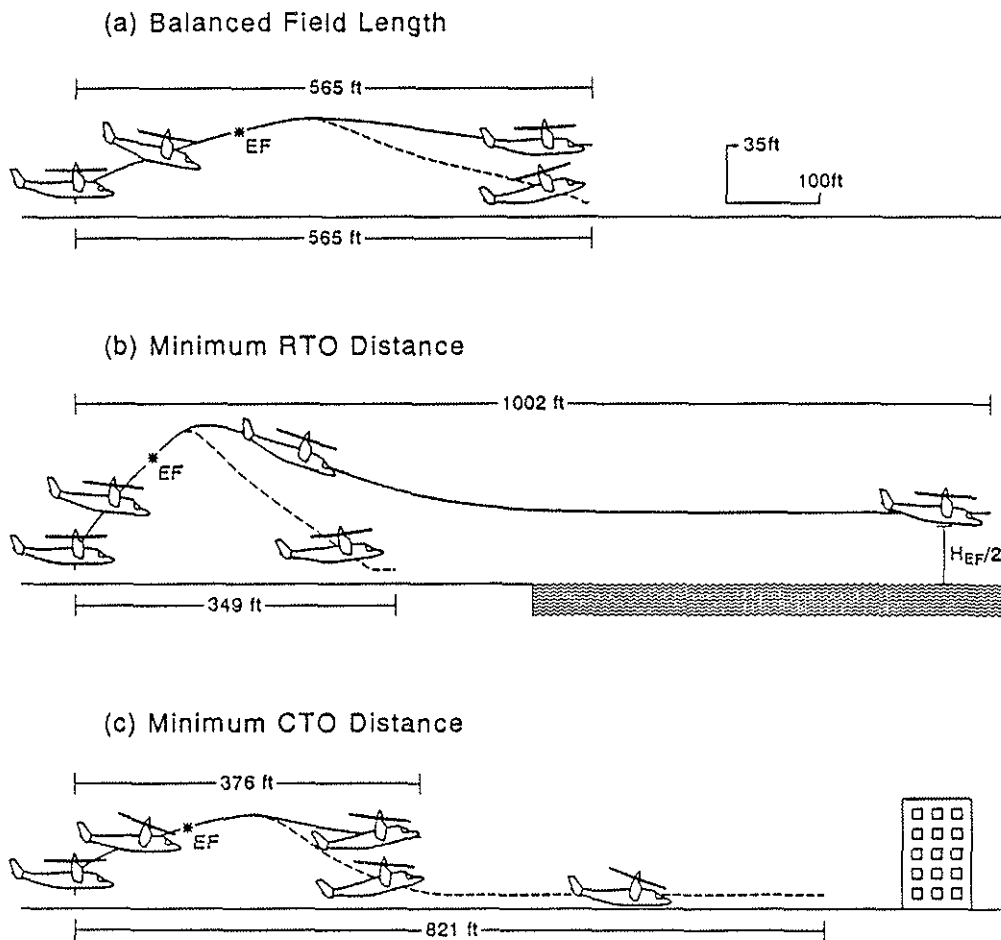
(a) Balanced Field Length

(b) Minimum RTO Distance

(c) Minimum CTO Distance

Fig. 8 Optimal takeoff procedures for various takeoff field configurations (W=12870 lbf).
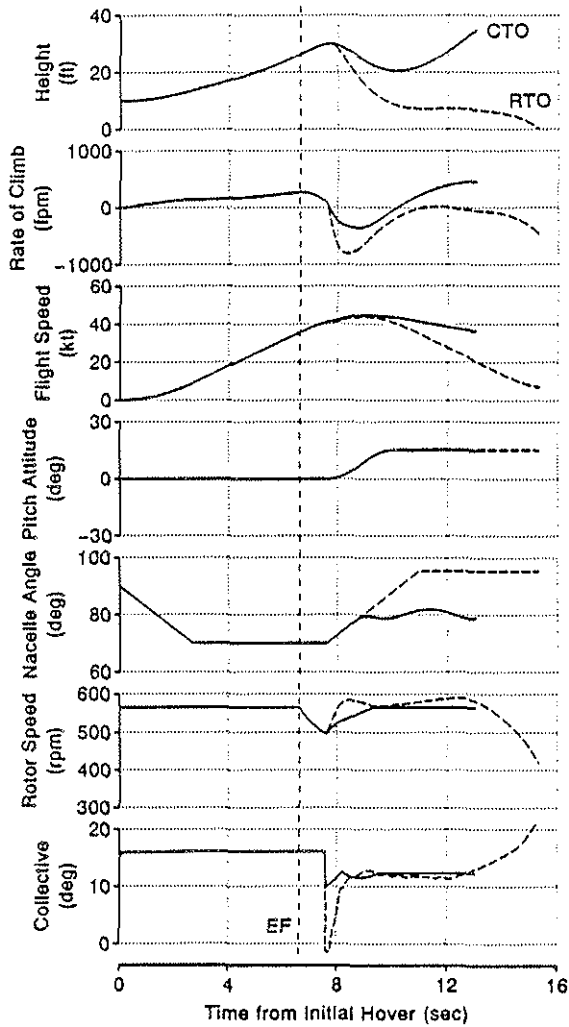
Fig. 9 Time histories of continued and rejected takeoffs with optimal nacelle angle control (W=13500 lbf).

When the required takeoff distance is within the available takeoff field length, the maximum takeoff weight for the conversion mode oblique takeoff is limited by the AEO hover ceiling, whereas the maximum takeoff weight for the helicopter mode oblique takeoff is normally limited by the OEI climb performance requirement due to the increase in necessary power caused by the negative pitch attitude.

Vertical Takeoff

A vertical takeoff is usually performed at a low backward speed, and consequently requires eliminating the unsafe region in the H-V diagram, thereby resulting in a significant takeoff weight limitation. The optimization problem for VTOL operations is therefore formulated to maximize the takeoff weight using the terminal condition that the touchdown speed factor from the most critical landing height (i.e., the height at which the touchdown speed factor is at its maximum) is within the landing gear capacity. The performance index and the terminal conditions are

$$I = \min_{h(0)} \max m$$

where

$$h(t_f) = 0, \quad \{u(t_f)/u_{\max}\}^2 + \{w(t_f)/w_{\max}\}^2 \le 1$$

The critical decision height, the minimum height to continue takeoff following power failure, is determined by

$$I = \min h(0)$$

where

$$h(t_f) \ge 35 \text{ ft}, \quad w(t_f) \le 0, \quad u(t_f) \ge V_2$$

The optimal RTO path from the critical decision height was calculated so as to minimize the touchdown speed factor using the terminal condition of landing at the original takeoff point as follows:

$$I = \min \left[\{u(t_f)/u_{\max}\}^2 + \{w(t_f)/w_{\max}\}^2 \right]$$

where

$$h(t_f) = 0, \quad x(t_f) = 0$$

Here the resultant touchdown speed factor is usually within the landing gear capacity since the critical decision height is much higher than the most critical landing height.

Figure 10 shows the optimal CTO and RTO paths, where the horizontal distance between the CDP and the takeoff point is determined so that the termination of the CTO is just above the takeoff point in order to obtain an exact zero-field-length operation. In actual operations, however, the horizontal location of the CDP should be determined so that the pilot can keep the landing site within sight since the CTO path is not as restricted.

Running Takeoff

The nacelle angle during the running takeoff was assumed to be constant and determined so as to maximize the takeoff weight, being limited by the OEI climb performance requirement. The critical decision speed, the rotation speed, and the pitch attitude after rotation were also assumed to be constant, and then determined to minimize the required takeoff distance.
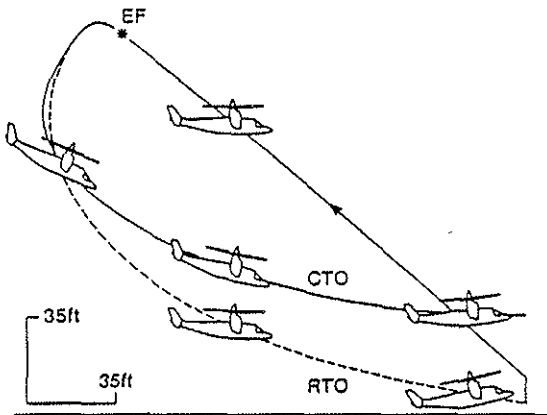

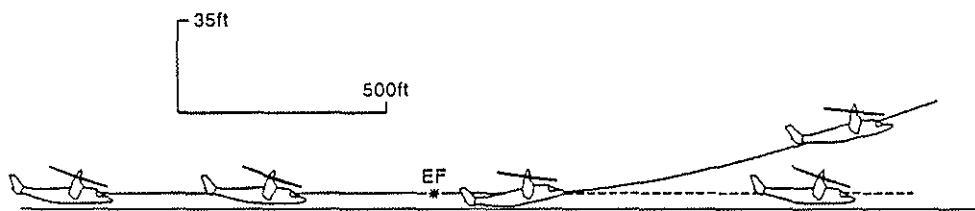Fig. 10 Optimal continued and rejected takeoff paths for a vertical takeoff (W=11470 lbf).

Figure 11 shows the optimal CTO and RTO paths for the minimum required takeoff distance. It should be noted that the BFL condition is not realized because its critical decision speed is higher than that at which the CTO distance is minimum, hence the BFL is longer than this minimum required takeoff distance.

Optimal Takeoff Procedures

Figure 12 (a) and (b) summarize each takeoff procedure's minimum required takeoff distances and maximum takeoff weight obtained in the preceding sections. The optimal takeoff procedures according to the available takeoff field length and the resultant maximum takeoff weight are concluded to be as follows: 1) Zero-filed-length operations allow a 11500 lbf maximum takeoff weight, 2) A 600 foot takeoff field allows a 13000 lbf takeoff weight using either a helicopter or conversion mode takeoff, although if the nacelle angle is optimally controlled following power failure, an additional 500 lbf is allowed, and 3) If a 2000 foot runway is available, any takeoff weight within the design limit is allowed. It should be noted that these results are based on the following assumptions: 1) Sea level, 20°C OAT, 2000 shp AEO and 1250 shp OEI power, 2) Required takeoff distance is defined as the longer of the CTO and RTO distances, and 3) The critical decision speed is optimized for each operational condition so that the BFL condition is obtained.

Fig. 11 Optimal continued and rejected takeoff paths for a running takeoff (W=16320 lbf).

Fig. 12 Variation of required takeoff distances with respect to takeoff weight for various takeoff procedures.

Conclusion

Nonlinear optimal control theory was successfully applied to tiltrotor aircraft control following power failure. Optimization of the various takeoff procedures, i.e., vertical, running, and oblique takeoffs in either helicopter or conversion mode, corresponding to the available takeoff field length, showed distinct advantages in increasing the maximum takeoff weight, especially when applying variable critical decision speeds according to the takeoff field configuration. The results obtained here are expected to contribute to the efficient use of tiltrotor aircraft in transport category operations, with the presented theory being considered to be useful in reducing the cost, time, and risks involved in the certification flight tests.

References

[1] "Interim Airworthiness Criteria, Powered-Lift Transport Category Aircraft," Department of Transportation, Federal Aviation Administration, July, 1988.

[2] Okuno, Y., Kawachi, K., Azuma, A., and Saito, S., "Analytical Prediction of Height-Velocity Diagram of a Helicopter Using Optimal Control Theory," *Journal of Guidance, Control, and Dynamics*, Vol. 14, No. 2, March-April 1991, pp. 453-459.

[3] Churchill, G. B. and Dugan, D. C., "Simulation of the XV-15 Tilt Rotor Research Aircraft," NASA TM 84222, March 1982.

[4] Dugan D. C., Erhart, R. G., and Schroers, L. G., "The XV-15 Tilt Rotor Research Aircraft," NASA TM 81244, September 1980.

[5] Jacobson, D. H., and Lele, M. M., "A Transformation Technique for Optimal Control Problems with a State Variable Inequality Constraint," *IEEE Transactions on Automatic Control*, Vol. AC-14, No. 5, October 1969, pp. 457-464.

[6] Wu, A. K. and Miele, A., "Sequential Conjugate Gradient Restoration Algorithm for Optimal Control Problems with Non-Differential Constraints and General Boundary Conditions, Part 1," *Optimal Control Applications and Methods*, Vol. 1, 1980, pp. 69-88.

Bibliography

[1] Martin, S., Jr., Erb, L. H., and Sambell, K. W., "STOL Performance of the Tilt Rotor," presented at the 6th European Rotorcraft and Powered Lift Forum, Bristol, England, September 1980.

[2] Sambell, K. W., "Conceptual Design Study of 1985 Commercial Tilt Rotor Transports, Volume III - STOL Design Summary," NASA CR-2690, April 1976.

[3] Marr, R. L. and Roderick, W. E. B., "Handling Qualities Evaluation of the XV-15 Tilt Rotor Aircraft," presented at the 30th Annual National Forum of the Am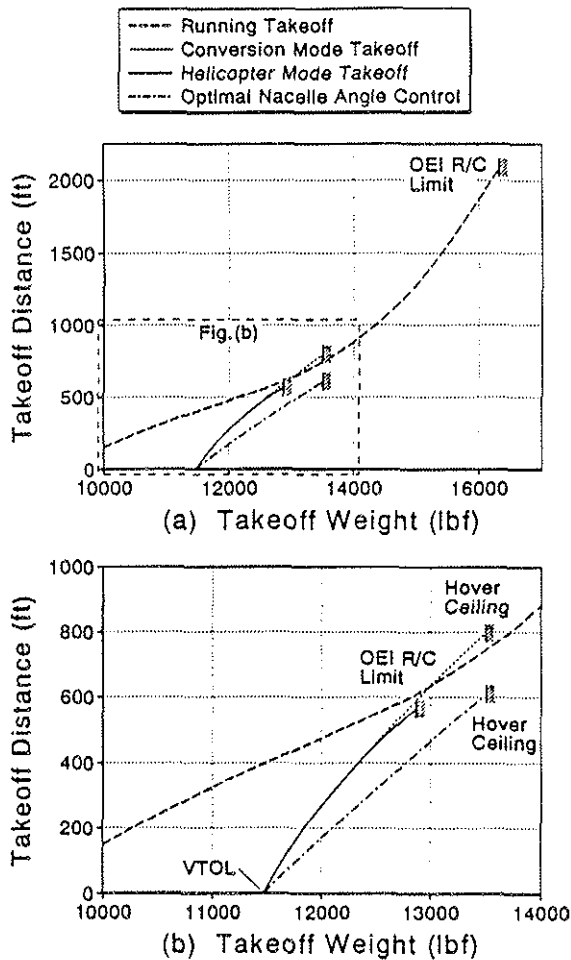erican Helicopter Society, May 1974.